Journal of Applied Polymer Science

The Conductive Network Made Up by the Reduced Graphene Nanosheet/Polyaniline/Polyvinyl Chloride

Feifei Ma,[1] Ningyi Yuan,[2] Jianning Ding[2]

[1]Jiangsu Key Laboratory for Solar Cell Materials and Technology, Changzhou 213164, Jiangsu, People's Republic of China
[2]Center for Low-Dimensional Materials, Micro-Nano Devices and System, Changzhou University, Changzhou 213164, People's Republic of China
Correspondence to: J. Ding (E-mail: dingjn@cczu.edu.cn)

ABSTRACT: In this work, due to the effective interfacial interactions between reduced graphene oxide (RGO) planes and polyaniline (PANI) chains, a conductive network was designed and fabricated by *in situ* polymerization of aniline monomer on the RGO planes. Then, the polyvinyl chloride (PVC) was modified with the conductive network by simple solution blending. A significant enhancement in the conductive properties of PVC films was obtained with a 4.0 wt % RGO and 7.0 wt % PANI loading. When the PANI was coated on RGO, the PANI was easier to connect mutually and enhanced the conductivity network for composites. Thermal analysis of the composite films showed the thermal stability of PVC was also improved after modified. © 2012 Wiley Periodicals, Inc. J. Appl. Polym. Sci. 128: 3870–3875, 2013

KEYWORDS: poly (vinyl chloride); functionalization of polymers; nanotubes; graphene and fullerenes; properties and characterization

Received 5 July 2012; accepted 19 September 2012; published online 12 October 2012
DOI: 10.1002/app.38624

INTRODUCTION

In recent years graphene, consisting of one- or several-atom-thick two-dimensional (2D) graphite layers, has attracted considerable attention.[1] Individual graphene sheets show high values of thermal conductivity,[2] Young's modulus,[3] large surface area,[4] ballistic transport on submicron scales, and mass less Dirac fermions charge carrier abilities.[5,6] These properties make graphene a promising material for using in many applications such as photovoltaic devices, sensors, transparent electrodes, super capacitors, and conducting composites.[7–12]

Graphene as fillers for polymer matrix composites have shown a great potential for various important application. However, because graphene has a pronounced tendency to agglomerate in a polymer matrix, pristine graphene is unsuitable for intercalation by large species and does not form homogeneous composites. PANI is most likely chosen to be the conductive polymer backbone for RGO-polymer composites because of its ease of synthesis, excellent environmental stability, and many interesting chemical, electrical, and optical properties and also for its tremendous applicability in electronic, optical, and magnetic materials such as information storage, rechargeable batteries, electro chromic display devices, sensors, nonlinear optics, composites, field emission (FE) displays, etc.[13–16]

Covalent attachment is the only tool that allows us to prepare a composite with efficient filler/polymer interactions leading to composites with improved properties. In this article, we describe a series of experiments carried out to incorporate a conductive network into polyvinyl chloride (PVC) and to obtain composites with good electrical properties and thermal stability.

EXPERIMENTAL DETAILS

Materials

Flaky graphite with an average particle size of 45 μm was purchased from Qingdao Huatai Lubricant Sealing S&T (China). Ammonium peroxydisulfate (APS), sulfuric acid (H_2SO_4, 98%), hydrochloric acid (HCl), *N*-Methyl pyrrolidone (NMP), and aniline (ANI) were analytic grade and commercially available reagents, and dodecylbenzenesulfonic acid (DBSA) was technical grade. PVC in powder form (Mw 120,000) were purchased from Aldrich.

Preparation of RGO Powder

The experimental procedures for the preparation of graphene oxide (GO) sheets are described in detail as follows.[17,18] First, 2 g of flaky graphite with an average size of 45 μm, 2 g of $NaNO_3$, and 96 mL of concentrated H_2SO_4 were mixed at 0°C, and the mixture was continuously stirred using a magnet stirrer afterwards. Second, 12 g of $KMnO_4$ was gradually added into the above mixture at 0°C. The obtained mixture was first stirred at 0°C for 90 min and then at 35°C for 2 h. Third, distilled water (80 mL) was slowly dropped into the resulting solution to

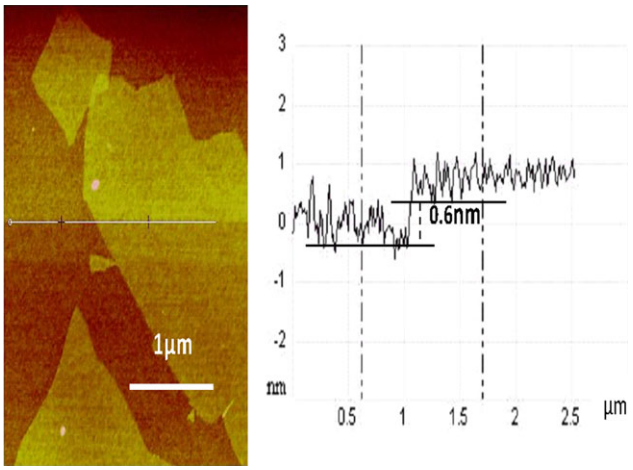

Figure 1. The AFM picture of RGO. [Color figure can be viewed in the online issue, which is available at wileyonlinelibrary.com.]

dilute the mixture in 30 min. Then 200 mL distilled water was added followed by 10 mL H_2O_2 (30%), and the stirring continued for additional 10 min to obtain a GO suspension. Finally, the residual permanganate and manganese dioxide were reduced to colorless soluble manganese sulfate by H_2O_2. The GO deposit was repeatedly washed with distilled water until the pH was close to neutral and then collected.

Thermal exfoliation of the resulting GO was achieved by placing it into a quartz tube with one sealed end. The other end of the quartz tube was closed using a rubber stopper, through which an argon inlet was then inserted. The sample was flushed with argon for 10 min. After that, it was quickly inserted into a Lindberg tube furnace preheated to 1050°C and kept for 30 s.[19]

In situ Polymerization of ANI Monomer in the Presence of RGO

PANI/RGO composites were prepared by *in situ* polymerization of ANI monomer in the presence of RGO. In a typical experiment, RGO was dispersed in NMP by sonication for 2 h. This suspension (2 mg/mL) was added to a reaction flask containing 30 mL of 1 *M* HCl solution, 0.93 g of DBSA, and 0.93 g of ANI. The mixture was stirred for 30 min and then another 30 mL of 1 *M* HCl solution containing 4.79 g APS was added dropwise to the mixture. The reaction mixture was kept under static conditions for 6 h at 0–5°C. After the reaction, the product was filtered, washed with distilled water followed by acetone, and dried in a vacuum oven at 65°C for 24 h.

Preparation of RGO/PANI/PVC Composites

The obtained RGO/PANI powder was grinded and dissolved in NMP with a concentration of 2% (RGO/PANI wt/NMP vol). Then, the solution was mixed with NMP solution of PVC (2%, PVC wt/NMP vol) in different ratios. After that, the mixed solutions were submitted to sonication for 3 h. Free-standing RGO/PANI/PVC composite films with a thickness of around 100–150 μm were prepared by casting the mixed solutions on glass plates and drying at 70°C under vacuum for 48 h.

Characterizations

To confirm RGO produced from GO through thermal exfoliation, Atomic force microscopic (AFM) images were recorded using Agilent AFM with Pico plus molecular imaging system in the noncontact mode. X-ray diffraction (XRD) analysis was performed with a Rigaku Dmax-2000 diffractometer using CuKa radiation. Raman measurements were performed on a Raman spectroscopy (DXR Raman microscope).The morphology of the RGO/PANI and RGO/PANI/PVC composites was examined with a scanning electron microscopy (SEM, Model JSM-6360LA) and a transmission electron microscope (TEM, HitachiH-8100). Fourier transforms infrared (FTIR) spectroscopy spectra were recorded on a Nicolet Avatar 370 FTIR spectrometer. The dc-conductivity of the samples was measured using a Keithley 2400 electrometer, and the ac-conductivity was measured over the frequency range from 100 Hz to 100 kHz using a LCR meter (model 819, Goodwill Instek). TGA (Q500, TA Instrument) was performed at a heating rate of 10°C min^{-1} from room temperature to 700°C under nitrogen gas condition.

RESULTS AND DISCUSSION

AFM Analysis

Samples for AFM images were prepared by depositing the corresponding solutions onto a freshly cleaved mica surface and allowing them to dry in air. Figure 1 displays the AFM image of RGO nanoakes, deposited onto the mica sheets from NMP suspension. AFM image indicated that the flakes were very small with dimensions of the order of less than 3 μm. The thickness was found to be of the order of 0.6 nm, corresponding to one to two graphene layers.

XRD Analysis

XRD patterns of PVC, RGO/PANI, and RGO/PANI/PVC composite are presented in Figure 2. XRD of pure PVC showed a broad peak in the region of 10–30°, showing the PVC has an amorphous structure. The RGO/PANI composite display a characteristic 2θ peak for the layered structure of graphene at around 25.4°, which corresponds to a layer-to-layer distance (d spacing) of about 0.35 nm, such an expansion of layer distance can be explained by the adsorption and intercalation of

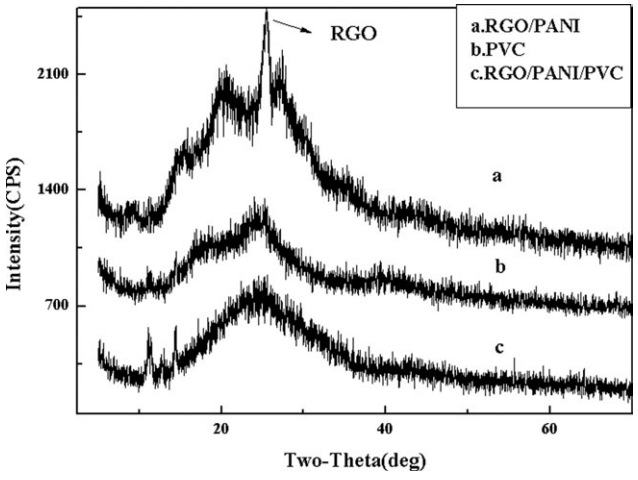

Figure 2. The XRD spectra of PVC, RGO/PANI, and RGO/PANI/PVC composite films.

Applied Polymer SCIENCE

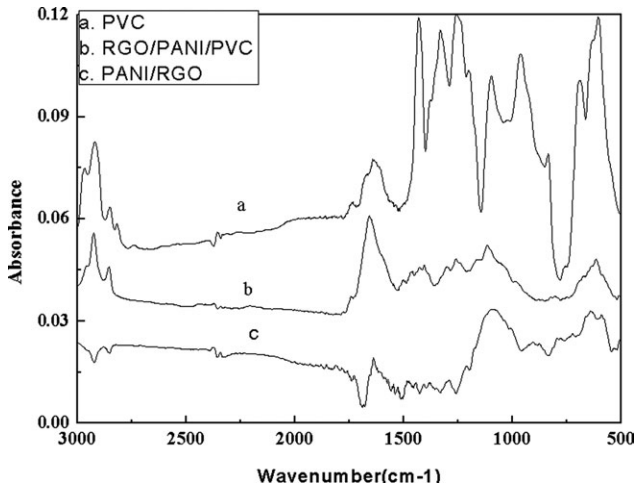

Figure 3. The FTIR spectra of PVC, RGO/PANI, and RGO/PANI/PVC composites.

the PANI on the surface and between the RGO sheets. The PANI is lack of obvious crystalline character which shows broad reflection peaks at $2\theta = 20.22°$ and 26.65°. Simultaneously, the peak at 25.4° cannot be detected for the sample with RGO/PANI/PVC, indicating that the reduced graphene sheets cannot stack with each other anymore to form crystalline structures if the coverage of PANI is densely enough.

FTIR Analysis

The FTIR spectroscopy is a powerful tool for analyzing the molecular structure of RGO/PANI/PVC composites. Figure 3 shows the FTIR spectra of PVC, RGO/PANI, and RGO/PANI/PVC composites. The band observed at 606 cm^{-1} is assigned to the C—Cl stretching in pure PVC.[20] The mixing of PANI in PVC causes this band to shift to lower wave numbers. The shifting of C—Cl band may be ascribed to the chemical interaction (strong dipole–dipole interaction) between C—Cl group of PVC and amine of PANI. The band observed at 2968 cm^{-1} is assigned to the stretching C—H of CHCl. The characteristic bands of PANI observed around 1561 and 1483 cm^{-1} in RGO/PANI and RGO/PANI/PVC composites correspond to the stretching of quinoid and benzoid rings, respectively.[21]

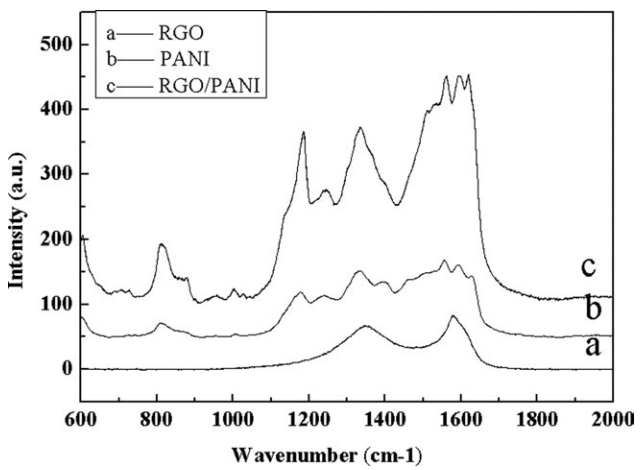

Figure 4. The micro-Raman spectra of the RGO, PANI, and RGO/PANI.

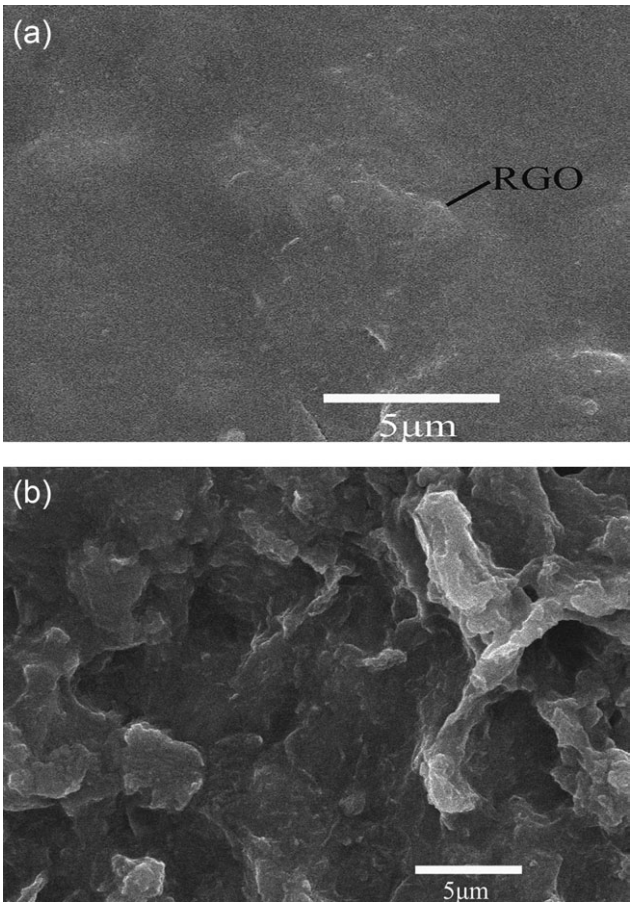

Figure 5. The SEM-images of the RGO/PVC (**a**) and RGO/PANI/PVC composite films (**b**).

Raman Analysis

The Raman spectroscopy was utilized to investigate chemical grafting of PANI polymers to the RGO surface using the RGO (Figure 4a), PANI (Figure 4b) and the composite of RGO/PANI (Figure 4c). The spectrum of RGO shows two dominant peaks at 1364 and 1580 cm^{-1}, corresponding to the D and G bands of graphene, respectively. The main bands situated at 1591, 1526, 1395, 1334, 1238, 1175, and 998 cm^{-1} is the characteristic bands of the PANI in Figure 4b. The spectrum of the RGO/PANI composite comprises the characteristic bands of both graphene and PANI. However, compared with the spectrum of RGO, the intensity ratio of the D to G bands (ID/IG) in the RGO/PANI composite decreases from 0.82 to 0.75. This finding indicates the influence of PANI on graphene due to the intimate interaction between them. Furthermore, the bands of RGO/PANI composite turn to blue shift clearly compared with that of pure PANI. For example, the peak at 1342 cm^{-1} shifts from 1334 cm^{-1}, the peak at 1185 cm^{-1} shifts from 1175 cm^{-1}, and the peak centered at 1002 cm^{-1} shifts from 998 cm^{-1}. These shifts demonstrate that the π–π interaction and hydrogen bonding between the RGO nanosheets and the PANI.

SEM and TEM Analyses

Figure 5 shows the SEM-images of the RGO/PVC and RGO/PANI/PVC composite films. It is found that the RGO/PVC

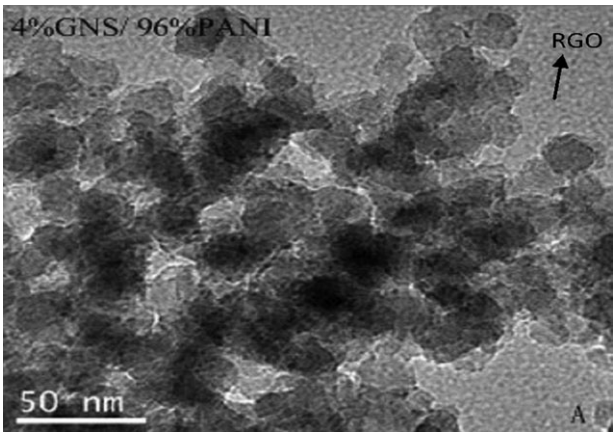

Figure 6. The TEM images of the RGO/PANI.

composite films have isolated island structures, whereas the RGO/PANI/PVC composite films appear a network structure. TEM images of the RGO/PANI composites (as shown in Figure 6) indicated that the reduced GO sheets are homogeneously surrounded with PANI and the PANI distribute both on the surface and between the RGO sheets. The PANI synthesized uniformly and formed spherical nanoparticles about 20 nm in size. Such good dispersion of the RGO/PANI structure into the PVC matrix may contribute to enhancing the electrical properties and molecular structure of composites. It is suggested that the good dispersion of the RGO/PANI structure in PVC matrix could enhance the surface-to-volume ratio and interfacial factors, which could on the whole contribute to potent electrical properties effect for the composites. Because of this especial structure, the interfacial affinity of the RGO/PANI with the PVC matrix increased and led to an ensured thermal stability and electrical contact that served as the electrically conductive network.

TGA

TGA is one of the thermal analysis techniques used to quantify weight change and thermal decomposition of the sample. TGA curves of the pure PVC resin and its composites loaded with RGO/PANI are shown in Figure 7a. For unfilled PVC sample it can be observed that there are two weight-loss stages (I and II). In the first stage the decomposition starts at about 242°C and ends around 375°C (stage I). During this first decomposition stage, the sample weight loss is due to the phenomenon of dehydrochlorination (HCl evolution).[22] Under the effect of temperature, chlorine radicals resulting from scission of —C—Cl labile bonds take off a hydrogen radical from adjacent —C—H groups to form a covalent H—Cl bond. This chemical mechanism induces double bonds along the polymer chain and may lead to conjugated polymeric chains. Indeed, after HCl evolution, conjugated double bonds are obtained and a new polymer, the polyacetylene, is formed. This polymer is more heat stable than PVC.[23–26] From 375°C to 515°C, a second decomposition stage is corresponding to polyacetylene cracking (scission of covalent and multiple bonds). Above 515°C, a stable residue is formed that corresponds to carbon black. In addition, seen from the derivative TGA (DTG) plots, the RGO/PVC and RGO/PANI/PVC composites are thermally more stable than that of PVC, as shown in Figure 7b. A shift of 15°C (from 460°C to 475°C) on decomposition temperature (T_d) is observed for RGO/PANI/PVC (4%/7%/89%). This enhancement on thermal stability is due to the presence of which RGO/PANI acts as barrier to minimize the permeability of volatile degradation products from the PVC composites. It is clear that the presence of filler increases the thermal stability of the PVC composites. The char yield of composites was found to be higher than those of unfilled PVC at higher temperatures.

Electrical Properties Analysis

The dc-conductivity values (σ_{DC}) of PVC-based composites with respect to the doping-amount of RGO and PANI are listed in Table I. In general, RGO is not compatible with organic polymers and very difficult to be dispersed in polymer matrixes because of their finer size and high aggregating tendency. In order to improve the dispersion of RGO in the PVC matrix, *in situ* polymerization of ANI monomer in the presence of RGO was adopted. Therefore, the functional groups can favor the chemical grafting of PANI polymers to the RGO surface in the *in situ* polymerization, which may assist in the preparation of

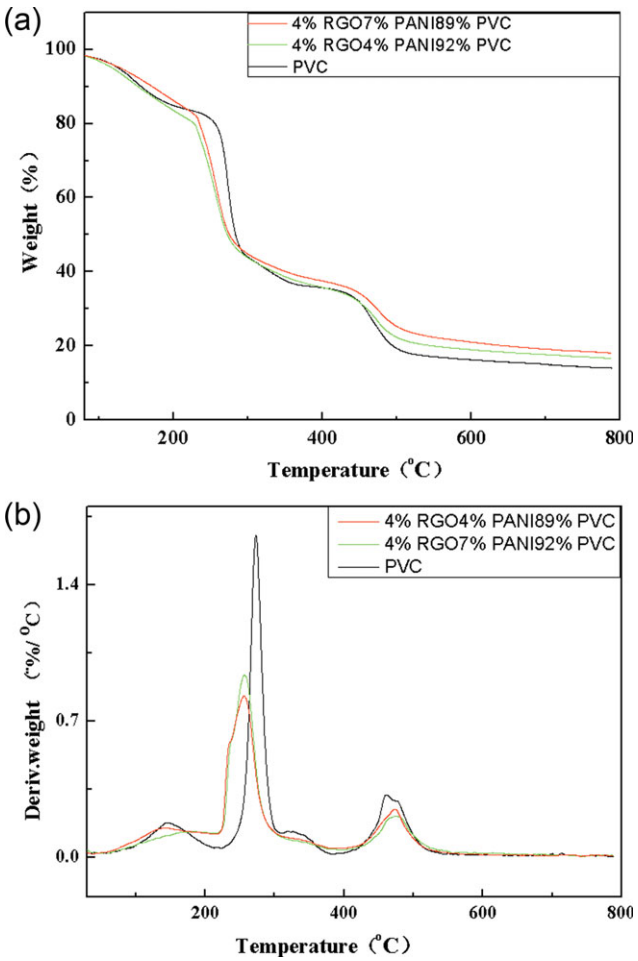

Figure 7. The TGA plots (**a**) and DTG plots (**b**) of PVC and RGO/PANI/PVC composites. [Color figure can be viewed in the online issue, which is available at wileyonlinelibrary.com.]

Applied Polymer SCIENCE

Table I. The Dc-Conductivity of PVC-Based Composite Films

Sample	Wt % of PVC	Wt % of RGO	Wt % of PANI	Conductivity (s cm^{-1})
PVC	100	0	0	7.4×10^{-15}
PANI	0	0	100	0. 35
5%PANI/95%PVC	95	0	5	8.38×10^{-9}
10%PANI/90%PVC	90	0	10	1.70×10^{-6}
20%PANI/80%PVC	80	0	20	6.75×10^{-4}
1%RGO/99%PVC	99	1	0	3.81×10^{-9}
2%RGO/98%PVC	98	2	0	5.42×10^{-7}
4%RGO/96%PVC	96	4	0	3.51×10^{-4}
5%RGO/95%PVC	95	5	0	2.27×10^{-3}
6%RGO/94%PVC	94	6	0	9.48×10^{-3}
1%RGO/5% PANI/94%PVC	94	1	5	1.80×10^{-7}
2%RGO/5% PANI/93%PVC	93	2	5	7.68×10^{-5}
1%RGO/10% PANI/89%PVC	89	1	10	8.84×10^{-5}
2%RGO/10% PANI/88%PVC	88	2	10	1.21×10^{-3}
4% RGO/7% PANI/89%PVC	89	4	7	7.20×10^{-2}

well-dispersed graphene-based polymer composites. The PANI chains may link the individual RGO sheets and result in a high-conductivity network. It is observed that co-doping of RGO and PANI is more favorable to increase the conductivity than mono-doping of RGO or PANI. Moreover, when the doping amount of RGO and PANI reaches 4.0 wt % and 7.0 wt %, respectively, the composite's conductivity reaches the largest value of 7.20×10^{-2} S cm^{-1}, which would be due to formation of RGO plane-PANI chain conducting networks in PVC matrix.

The conducting network of PANI chains and RGO planes in PVC matrix is confirmed by the ac-conductivity measurements. The ac-conductivity of the composites with different doping ratio of RGO and PANI was studied with respect to frequency as shown in Figure 8. The relation between the ac-conductivity and frequency was represented by the eq. (1).[27–29]

$$\sigma_{AC} = \sigma_{DC} + 2\pi f \varepsilon' \quad (1)$$

where σ_{AC} is the ac-conductivity, σ_{DC} is the dc-conductivity, f is the measurement frequency, and ε' is the loss factor.

For the RGO/PVC and PANI/PVC composites, their σ_{AC} is frequency-dependent when the doping concentration of RGO below 2.0 wt %, respectively, which indicates that the continuous conductive network may not be properly formed for this low doping concentration in these composites. However, for the RGO/PANI/PVC composite, their σ_{AC} shows frequency-independence when the doping concentration of RGO and PANI reaches 1.0 wt % and 5.0 wt %, respectively. The result

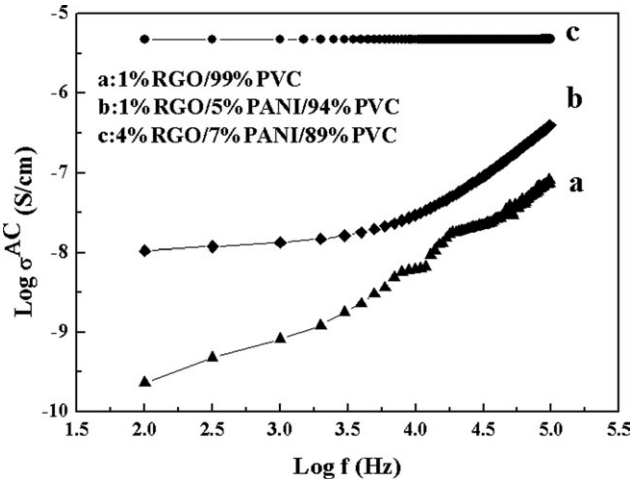

Figure 8. The variations of ac-conductivity of PVC-based composites against the frequency at different concentration of RGO and PANI.

demonstrates that the RGO/PANI/PVC composites need lower doping concentration of RGO or PANI than that in RGO/PVC or PANI/PVC to generate the continuous conductive network, which may be ascribed to the synergetic effect between RGO and PANI. Moreover, the RGO (4.0 wt %)/PANI (7.0 wt %)/PVC (89 wt %) composite shows frequency-independence even at high frequency region (100 kHz). This phenomenon proves that increasing the doping concentration of RGO in RGO/PANI/PVC composites can further improve the conductive networks in the insulating polymer matrix-PVC.

CONCLUSION

From the above study it could be concluded that: the conductivity of PVC was dramatically enhanced (i.e., 7.2×10^{-2} Scm^{-1}) by filling the host polymer with RGO and PANI at low concentration (i.e., 4.0 wt % and 7.0 wt %, respectively). The characterizations reveal that the RGO disperses well in the polymer matrix, and A 3D network of conductive composed of RGO planes and PANI chains was also formed, which may be ascribed to formation of PANI grafting polymer chains on the RGO planes in *situ* polymerization. On the other hand, thermal stability of the RGO/PANI/PVC composites is also improved. The present research introduces a novel material with potential applications in electromagnetic shielding, antistatic coatings, and corrosion-resistant coatings but the availability of processable graphene sheets in large quantities is crucial for its applications in composites.

ACKNOWLEDGMENTS

This work was financially supported by the Priority Academic Program Development of Jiangsu Higher Education Institutions, a grant from the National High Technology Research and Development Program of China (863 Program) (2011AA050511), Jiangsu "333" Project (201041).

REFERENCES

1. Salavagione, H. J.; Martínez, G.; Ellis, G. *Macromolecular* **2011**, *22*, 1771.
2. Balandin, A. A.; Ghosh, S.; Bao, W.; Calizo I.; Teweldebrhan D.; Miao, F. *Nano Lett.* **2008**, *8*, 902.
3. Lee, C.; Wei, X. D.; Kysar, J. W.; Hone, J. *Science* **2008**, *321*, 385.
4. Stoller, M. D.; Park, S. J.; Zhu, Y. W.; An, J. H.; Ruoff, R. S. *Nano Lett.* **2008**, *8*, 3498.
5. Zhang, Y. B.; Tan, Y. W.; Stormer, H. L.; Kim, P. *Nature* **2005**, *438*, 201.
6. Novoselov, K. S.; Geim, A. K.; Morozov, S. V.; Jiang, D.; Katsnelson, M. I.; Grigorieva, I. V. *Nature* **2005**, *438*, 197.
7. Liu, Z. F.; Liu, Q.; Huang, Y.; Ma, Y. F.; Yin, S. G.; Zhang, X. Y. *Adv. Mater.* **2008**, *20*, 3924.
8. Robinson, J. T.; Perkins, F. K.; Snow, E. S.; Wei, Z. Q.; Sheehan, P. E. *Nano Lett.* **2008**, *8*, 3137.
9. Ang, P. K.; Chen, W.; Wee, A. T. S.; Loh, K. P. *J. Am. Chem. Soc.* **2008**, *130*, 14392.
10. Wu, J. B.; Becerril, H. A.; Bao, Z. N.; Liu, Z. F.; Chen, Y. S. *Appl. Phys. Lett.* **2008**, *92*, 263302.
11. Stankovich, S.; Dikin, D. A.; Dommett, G. H. B.; Kohlhaas, K. M.; Zimney, E. J.; Stach, E. A. *Nature* **2006**, *442*, 282.
12. Yousefi, N.; Gudarzi, M. M.; Zhang, Q. B.; Aboutalebi, S. H.; Sharif, F.; Kim, J. K. *J. Mater. Chem.*, **2012**, *22*, 12709.
13. Alexander, P.; Nikolay, O.; Alexander, K.; Galina, S. *Prog. Polym. Sci.* **2003**, *28*, 1701.
14. Pedro, G. R. *Adv. Mater.* **2001**, *13*, 163.
15. Cao, Y.; Smith, P.; Heeger, A. J. USPat.5,232,631, **1993**.
16. Ding, S.; Chao, D.; Zhang, M.; Zhang, W. *J. Appl. Polym. Sci.* **2008**, *107*, 3408.
17. Singh, V.; Joung. D.; Seal S. *Prog. Mater. Sci.* **2011**, *56*, 1178.
18. Kuilla, T.; Bhadra, S.; Lee, J. H. *Prog. Polym. Sci.* **2010**, *35*, 1350.
19. McAllister, M. J.; Li, J. L.; Douglas, H.; Car, R. A.; Aksay. I. A. *Chem. Mater.* **2007**, *19*, 4396.
20. Beltran, M.; Marcilla, A. *Eur. Polym. J.* **1997**, *33*, 1135.
21. Afzal, A. B.; Akhtar, M. J.; Nadeem, M.; Ahmad, M.; Hassan, M. M.; Yasin, T.; Mehmood, M. *J. Phys. D Appl. Phys.* **2009**, *42*, 015411.
22. Djidjelli, H.; Sadoun, T.; Benachour, D. *J. Appl. Polym. Sci.* **2000**, *78*, 685.
23. Li, B. *Polym. Degrad. Stab.* **2000**, *68*, 197.
24. Benavides, R.; Castillo, B. M.; Castañeda, A. O.; López, G. M.; Arias, G. *Polym. Degrad. Stab.* **2001**, *73*, 417.
25. Conesa, J. A.; Molto, J.; Font, R.; Egea, S. *Ind. Eng. Chem. Res.* **2010**, *49*, 11841.
26. Bishay, I. K.; Abd-El-Messieh, S. L.; Mansour, S. H. *Mater. Des.* **2011**, *32*, 62.
27. Barrau, S.; Demont, P.; Peigney, A.; Laurent, C.; Lacabanne, C. *Macromolecules* **2003**, *36*, 5187.
28. Leyva, M. E.; Barra, G. M. O.; Moreira, A. C. F.; Soares, B. G.; Khastgir, D. *J. Polym. Sci. Polym. Phys.* **2003**, *41*, 2983.
29. Dang, Z. M.; Nan, C. W.; Xie, D.; Zhang, Y. H.; Tjong, S. C. *Appl. Phys. Lett.* **2004**, *85*, 97.